Using Chirplet Chains for a Chirplet-Omega Search a Trigger Clustering Algorithm

Zachary Nemtzow*, Éric Chassande-Mottin†, Satya Mohapatra* and Laura Cadonati*

**Physics Department, University of Massachusetts, Amherst MA 01003 (USA)*

† *CNRS and Univ. Paris Denis Diderot,*

AstroParticule et Cosmologie (France)

Gravitational waves are one of the many astrophysical messengers with which we can learn about our universe. Although no valid detection has been made to date, gravitational waves from the coalescence of massive bodies is projected to be a promising source for potential detection. We examine a method for improving the chirplet omega pipeline sensitivity to binary coalesence that are extended in time in forming *chirplet chains*. By appropriately clustering the variant frequency sin-gaussian pixels the algorithm uses to decompose the data, the signal to noise ratio SNR of events can be greatly increased. We present such a clustering method and discuss means of testing its performance.

I. INTRODUCTION

The subject of gravity has piqued the minds of physicists since Newton was hit on the head by an apple. In 1915, Albert Einstein's Theory of General Relativity replaced Newtons law of universal gravitation proclaiming that gravity was not merely a force emanating from particles with mass, but rather a property of space-time. Similar to the creation of electromagnetic waves in order to mediate motions of charges, gravitational waves are ripples in space-time that are produced to mediate changes in gravity fields caused by accelerated masses. The existence of gravitational waves has been indirectly substantiated by University of Massachusetts Amherst's own Hulse and Taylor [1, 2]. Using a radio telescope, the two scientists discovered and analyzed a binary pulsar, showing that its' orbit was decreasing in radius and loosing energy in strong agreement with that predicted by general relativity and gravitational waves.

Many scientific endeavors that aimed at the first direct detection of these elusive waves

have been born over the years. Ranging from large metal columns to spuper-cooled spheres, no valid detection has been made to date by any detector. However, the property that gravitational waves cause distortions in space-time perpendicular to their direction of propagation in a linear combination of two orthogonal polarizations seperated by 45°, h_+ ('h–*plus*') and $h_\times$ ('h–*cross*'), makes large scale interferometers a propitious tool to use in pursuit of gravitational waves detection. Already proving useful in such revolutionary undertakings as disproving the existence of the æther in favor of special relativity, Michelson-Morley interferometers are now conspiring with many other groundbreaking technologies to further corroborate Einstein's predictions.

Interferometers are used to measured relative changes in time it takes a photon to travel between two test masses placed at the end of two orthogonal arms. The quantity measured $h(t)$, called *starin*, is given by

$$h(t) = F_+ h_+(t) + F_\times h_\times(t)), \tag{1}$$

where the angular response of the detectors to the position and polarization of the detector, F_+ and $F_\times$, are given by

$$F_+ = 1(1 + cos_2\theta)cos_2\phi cos_2\psi + cos\theta sin2\phi sin2\psi, \tag{2a}$$

$$F_+ = -1(1 + cos_2\theta)cos_2\phi cos_2\psi + cos\theta sin2\phi sin2\psi. \tag{2b}$$

Here, θ is the altitude coordinate ranging from 0 to π with zero as the zenith, ϕ is the azimuth coordinate ranging from 0 to 2π, and ψ, ranging from 0 to π, determines the alignment of the polarization of the incoming wave to lines of constant θ and ϕ. The detector response is therefore at a maximum on the axis of the zenith with sensitivity of zero on the plane of the interferometer located 45° from the orthogonal arms.

Today, six major large-scale interferometers work in collaboration with the ultimate goal of the first detection of gravitational waves. The Laser Interferometer Gravitational Waves Observatory (LIGO) operates three Fabry-Perót Michealson interferometers at two sites, one in Hanford, Washington, and the other at Livingston, Louisiana. Both sites have detectors with arm lengths of 4km, and the Hanford site also operates a second half length detector. Similar to LIGO, Virgo is a 3km French-Italian detector located in Cascina, Italy, GEO600 is a 600m British-German detector located in Germany, and TAMA is a 300m detector located in Japan being used as a prototype for the planned Large Scale Cryogenic Gravitational Wave

Telescope (LCGT). In order to learn from one another and obtain a more credible detection, scientists from all projects work together in improving their instruments, and analyzing data. This global network of gravitational waves detectors will not only help validate a coincident event in many detectors as a detection, but will also help in the reconstruction of the waveform, parameters, and sky position of the event's source.

Current interferometric detectors observe a much larger bandwidth than previous detection pursuits and are much more sensitive, capable of measuring relative distance changes in arm length on the order of $10-^{-21}$. Although this translates measuring length distortion three orders of magnitude less than the diameter of a proton, space-time is quite stiff, and this achievement is not yet sensitive enough to see an event. The insufficient sensitivity is attributed to noise within the detectors.

The dominate sources of this limiting noise are seismic activity near the detectors, thermal vibrations in components of the instruments, and the photon shot noise. For this reason, some detectors are undertaking a multitude of upgrades to reduce detector noise from the many identifiable sources. Said upgraded detectors, to be called Advanced LIGO and Advanced Virgo, will hopefully improve sensitivity to within the range of detectable events. Additionally, a space-based detector is currently in the planning phases, with an uncertain future due to budgetary issues. With its' larger scale and isolation from earth-based noise sources from which current detectors suffer, this new detector promises substantial sensitivity and bandwidth improvements over current terrestrial detectors.

II. SEARCH ALGORITHMS

All these developments present a challenge to gravitational waves data analysts around the world to ready search algorithms for the approaching age of plausible detection. Moreover, development of these analysis techniques does not merely center around detection. Rather, many methods strive to ascertain information about event sources from the gravitational wave data. These endeavors will help add gravitational waves to the list of messengers, like electromagnetic waves and neutrinos, that scientists can use to cultivate knowledge about our universe. However, unlike other astronomical messengers, gravitational waves travel to earth virtually unobstructed, with detailed information about the cosmic movements of masses from which they originated. This provides scientists with the opportunity to learn

about the details of phenomena that are unobservable by other methods. This new messenger may even prove useful in discovering completely new information about our universe that has never before been observed nor predicted.

There are many types of astronomical events for which data analysts hope to make detections. These events are generally grouped into four major categories: burst, continuous, inspiral, and stochastic. They can be caused by energetic explosions, the rotation of irregularly shaped stars, binary system coalescence, and noise from the big bang respectively. Different search algorithms have been tailored to the distinct features that these sources may produce in the detector signal. In this paper, we will focus on a matched filter burst search called the Omega pipeline [3] and its variant, chirplet-omega.

A. Omega pipeline

The Omega pipeline is a burst search algorithm designed for the detection gravitational wave transients from sources that are unmodeled, and therefore, do not have enough template waveforms to form a *matched filter* search and would create too great computational costs to utilize *cross-correlation* techniques. Such sources include the merger phase of compact binary coalescence, core collapse of supernovae, etc. All of these processes produce rapid (often relativistic) movements of large quantities of mass.

The Omega pipeline follows an *abstract bases* approach whereby the data is decomposed into a bases of waveforms appropriate for the desired signal space. These waveforms can also be used to check for coincident events the data streams multiple detectors. In general, other like algorithms use either time-domain or time-frequency searches in the form of delta function or wavelets respectively. The basis used by omega is a multi resolution basis of complex waveforms that is over complete, producing minimum time-frequency uncertainty in order to improve the detection of signals at the cost of signal reconstruction. We follow the derivation of the bases functions in [3].

The burst signals Omega is designed to detect have time-domain and frequency-domain representation expressed by the Fourier pair

$$h(t) = \int_{-\infty}^{+\infty} \tilde{h}(f) e^{+i2\pi ft} \mathrm{d}f, \tag{3a}$$

$$\tilde{h}(f) = \int_{-\infty}^{+\infty} h(t) e^{-i2\pi ft} \mathrm{d}t, \tag{3b}$$

with the dimensionless strain amplitude is given by

$$||h|| = \int_{-\infty}^{+\infty} |h(t)|^2 \mathrm{d}t = \int_{-\infty}^{+\infty} |\tilde{h}(f)|^2 \mathrm{d}f. \tag{4}$$

The time and frequency domain can be normalized to give

$$\psi(t) = \int_{-\infty}^{+\infty} \tilde{\psi}(f) e^{+i2\pi ft} \mathrm{d}f, \tag{5a}$$

$$\tilde{\psi}(f) = \int_{-\infty}^{+\infty} \psi(t) e^{-i2\pi ft} \mathrm{d}t, \tag{5b}$$

with normalized strain amplitude $||\psi||$ (defined the same way as for $||h||$) equal to unity. Therefore the gravitational wave signal is defined by its strain amplitude multipled by the normalized Fourier pair

$$h(t) = ||h||\psi(t), \tag{6a}$$

$$\tilde{h}(f) = ||\tilde{h}||\tilde{\psi}(f). \tag{6b}$$

From this the central time, central frequency, duration and bandwidth can be defined as

$$\tau = \int_{-\infty}^{+\infty} t|\psi(t)|^2 \mathrm{d}t, \tag{7a}$$

$$\phi = \int_{0}^{+\infty} f|\tilde{\psi}(f)|^2 \mathrm{d}f, \tag{7b}$$

$$\sigma_t^2 = \int_{-\infty}^{+\infty} (t-\tau)^2|\psi(t)|^2 \mathrm{d}t, \tag{7c}$$

$$\sigma_f^2 = \int_{0}^{+\infty} (f-\phi)^2|\tilde{\psi}(f)|^2 \mathrm{d}f, \tag{7d}$$

respectively, and the dimensionless quality factor is defined as the ratio of the central frequency to the bandwidth

$$Q = \frac{\phi}{\sigma_f}. \tag{8}$$

Using the fact that the duration and bandwidth must obey the uncertainty relation

$$\sigma_t \sigma_f \geq \frac{1}{4\pi} \tag{9}$$

one can derive the resulting basis of complex valued sin-gaussians in each domain

$$h(t) = ||h(t)|| \left(\frac{1}{2\pi\sigma_t^2}\right)^{1/4} exp\left[-\frac{(t-\tau)^2}{4\sigma_t^2}\right] exp\left[i2\pi\phi\,(t-\tau)\right], \tag{10a}$$

$$\tilde{h}(t) = ||h(t)|| \left(\frac{1}{2\pi\sigma_f^2}\right)^{1/4} exp\left[-\frac{(f-\phi)^2}{4\sigma_f^2}\right] exp\left[i2\pi\tau\left(f-\phi\right)\right], \tag{10b}$$

allowing for arbitrary phase of the incoming gravitational wave. Finally this can then be normalized and expressed in terms of Q to give

$$\psi(t;\tau,\phi,Q) = \left(\frac{8\pi\phi^2}{Q^2}\right)^{1/4} exp\left[-\left(\frac{4\pi^2\phi^2}{Q^2}\right)(t-\tau)^2\right] exp\left[i2\pi\phi\left(t-\tau\right)\right], \tag{11a}$$

$$\tilde{\psi}(f;\tau,\phi,Q) = \left(\frac{Q^2}{8\pi\phi^2}\right)^{1/4} exp\left[-\left(\frac{Q^2}{4\pi^2\phi^2}\right)(f-\phi)^2\right] exp\left[i2\pi\tau\left(f-\phi\right)\right]. \tag{11b}$$

In order to appropriately tile the desired signal space, two priorities have taken into account. First, the basis must be complete enough to ensure small energy loss when matching basis functions to a signal, and second, it must not be too fine such that the computational cost becomes too high. Hence, a minimum mismatch, μ_{max}, is defined the maximum distance that a signal can be from its nearest eight templates in the signal space (imagine it being in the center of a cube, equidistant from all eight tiles at the corners). From this, the minimum distance between each template, δs_{max}, is defined as

$$\delta s_{max} = 2\left(\frac{\mu_{max}}{3}\right)^{1/2}. \tag{12}$$

which can be used to find the required τ, ϕ, and Q for the basis functions. By creating discrete Q-planes, discrete central frequencies, and central times can be determined to create the final tiling structure. For a depiction of the tiling space see Figure 1.

Once the space is tiled and data decomposed into waveform signals, a thresholding algorithm selects the tiles with the highest energy and therefore the closest match to the data, then an exclusion algorithm removes any overlapping tiles.

In order to improve this process, before decomposing the signal, the pipeline first employs a linear predictor error filter to whiten the raw data. This requires the assumption that the raw data is an autoregressive process, or that the detector environment in which the data is created acts as a filter itself, responding in a predictive way to the initial white noise signal input. A given predictable sequence $\tilde{x}[n]$ can be expressed in terms of the previous M samples by

$$\tilde{x}[n] = \sum_{m=1}^{M} c[m]x[n-m] \tag{13}$$

where the coefficients $c[m]$ are determined by training the filter on a a previous segment. After this training, the algorithm removes artifacts of correlated noise in the following samples

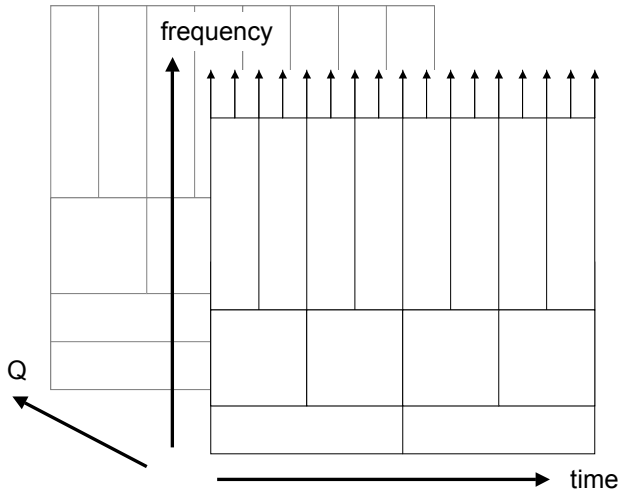

FIG. 1: Depiction of the signal space tiling structure of the Omega pipeline

of data yielding whitened data. Due to the computational cost of whitening large segment lengths, the omega search implements a finite impulse response filter in the frequency domain that uses cycles of fast Fourier transforms to reduce the computational cost from polynomial to logarithmic time.

This technique poses a problem when running coincident searches with multiple detectors, or coherent searches. That is, the dispersion of whitened data from different detectors may vary substantially, which will result in timing errors between the data sets. If the shift nears or surpasses the amount of time it takes gravitational waves of speed c to travel between detectors, the algorithm may dismiss an event because it is not properly observed in multiple detectors. To compensate for this potential problem, the omega search implements zero-phase filtering such that both the impulse response filter and its time reverse filter are applied to the data. When combined, this symmetry creates a zero-phase filter. The resultant filter can be expressed in the frequency domain as

$$Z(f) = B(f)B^*(f)X(f) \tag{14}$$

where $B(f)$ is the frequency domain response of the original filter expressed by its discrete time Fourier transform. With this whitened data stream, the Omega algorithm can increase

its sensitivity to burst gravitational waves sources.

B. Chirplet-omega Search Algorithm

One of the most promising sources of detectable gravitational waves is the coalescence of black hole and/or neutron star binaries. This coalescence is characterized by three phases, *inspiral*, *merger*, and *ringdown*. The first phase represents when two massive bodies are caught in one another's gravitational field, causing them to orbit one another. Just as in Hulse and Taylor's analysis of a binary containing a pulsar, the system looses energy in radiating gravitational waves hence causing the radius of the orbit to decrease over time and the orbital frequency to increase. As time progresses, the two bodies eventually spin close enough to collide, with rapid frequency evolution occurring both before and during the merger phase. Finally, the combined bodies emit gravitational waves as a the system settles in the ringdown phase. Although both the inspiral and ringdown phases are well modeled by various techniques, the merger phase still represents an unmodeled regime of burst gravitational waves. This phase also produces very high signal strength in the interferometer data.

The Omega pipeline is sensitive to parts of the inspiral and merger phases of coalescence, where the frequency may be changing quickly wilt respect to the duration of the templates. Ergo the assumption implied by the sin-gaussian basis family that the signal frequency evolution will be locally stationary may cause significant mismatch between the signal and the available templates. The chirplet-omega search algorithm is an extension of the omega pipeline that, in order to avoid such mismatch, adds a fourth parameter to the set of τ, ϕ, and Q, used by Omega, called chirprate d. This parameter governs the linear frequency variation

$$f(t) = \phi + d(t - \tau), ^{1}. \tag{15}$$

in the chirplet-like templates which when combined with Equation (11a) yields the normal-

[1] We follow the notation central time τ and central frequency ϕ set by [3] rather than that of [4]

ized time-domain chirplet templet definition

$$\psi(t;\tau,\phi,Q,d) = \left(\frac{8\pi\phi^2}{Q^2}\right)^{1/4} exp\left[-\left(\frac{4\pi^2\phi^2}{Q^2}\right)(t-\tau)^2\right] exp\left[i2\pi\left(\phi\,(t-\tau) + d\,(t-\tau)^2\right)\right]. \tag{16}$$

An example chirplet template is provided by Figure 2 with linear frequency evolution in Figure 3.

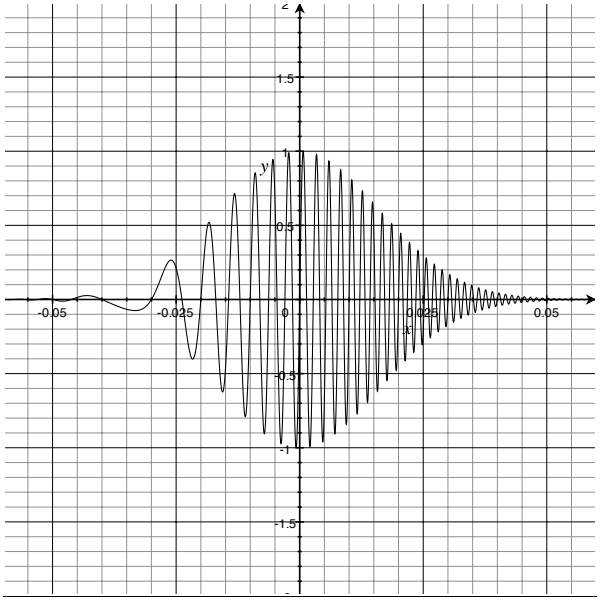

FIG. 2: Sin-gaussian template with $Q = 50,\ f = 350$, and $d = 5000$

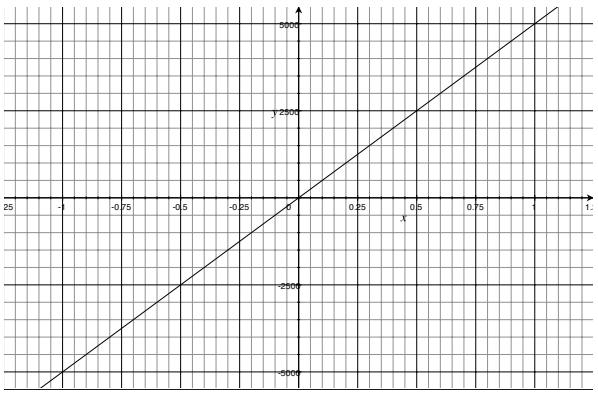

FIG. 3: Frequency evolution of chirprate $d = 5000$

In order to tile the desired signal space, a similar minimum mismatch technique is im-

plemented in the four dimensional space. However, this yields a number that is an order of magnitude larger than that required by standard Omega to tile a similar space with three parameters. Hence, the computational cost, which scales approximately linearly with the number of templates, will also increase by an order of magnitude. A consequence of the properties of the chirplet templates is that yields a much finer tiling of the low frequency space than does Omega, increasing its sensitivity to the detection of low coalescence frequencies of low mass binary systems. Previous studies have shown that this results in peak SNR recover of events by chirplet being between 5% to 40% higher than standard Omega.

III. CHIRPLET CHAINS

When attempting to separate a potential gravitational wave signal from the noise, two outcomes are possible. The first, H_0, being that there is in data x_k, there is only noise n_k, and the second, H_1, being that there is both signal s_k and noise present adding together to x_k. Although both Omega and the chirplet extension implement a whitening filter in order to reduce detector noise, some noise still remains in the data. Moreover, random (and thus not removed by the whitening filter) artifacts in the data may even appear to be H_1, yielding an energy tile with high significance, when they are are still just noise. With the knowledge that these false detections may occur, measures taken to avoid this may produce false dismissals, where H_0 is concluded when a signal exists. By using the Neyman-Pearson (NP) critereon, the error on the probability of a false dismisal can be minimized while keeping the false alarm probability fixed. The likelihood ratio follows this assumption and is defined as

$$\lambda = \frac{\mathbb{P}\left(\{x_k\}\right)|H_1}{\mathbb{P}\left(\{x_k\}\right)|H_0}, \tag{17}$$

and a given signal in the data,

$$s(t) = A cos\left(\phi(t) + \varphi_0\right), \tag{18}$$

the maximization of the likelihood ratio can be obtained for the amplitude A and instantaneous frequency φ_0. However, when attempting to maximize over t_0 and $\phi(t)$, it is computationally costly to maximize the likelihood over all possible smooth chirp phase evolutions over time. Therefore, it is convenient to discretize the phase evolution $\phi(t)$ as is done in

chirplet Omega. Hence, in order to recover the phase evolution of the smooth chirp signal, an approximation by means of a string of 'lines' can be implemented. The set of the resulting *chirplet chains* then forms a template grid of the set of smooth chirp signals. The measure of whether the phase evolution of the chirplet chain, ϕ^*, is a good approximation for that of the smooth chirp, ϕ , or the mismatch between the signal and chosen template, is given by

$$\mathcal{L}(\phi, \phi^*) = \frac{\ell(s;\phi) - \ell(s;\phi^*)}{\ell(s;\phi)}. \tag{19}$$

and should be less than the maximum mismatch defined in previous sections as μ_{max}. Minimizing this mismatch over the set of chirplet chains comes at a large computational cost. However, due to the fact that this mismatch is additive, dynamic programing can be implemented to split this large optimization problem into smaller ones. This is done by approximating smaller sections of a smooth chirplet by chirp templates, each minimizing the mismatch for a given section, and then connecting the templates to form a chirplet chain.

The connection processes is performed by connecting chirplet templates that satisfy *regularity constraints*. For the set of constant amplitude chirplet proposed in [5], there are absolute bounds for connecting two chirplets, N_r' and N_r'' defined as

$$|m_{j+1} - m_j| \leq N_r', \tag{20a}$$

$$|m_{j+1} - 2m_j + m_{j-1}| \leq N_r'', \tag{20b}$$

where m_j represents the time and frequency coordinate of the endpoint of the chirplet with m_{j-1} and m_{j+1} being similar coordinates for the chirplets before and after j in the chain. Through dynamic programming, the likelihood ratio becomes a sum over j chirp templates to create a chirplet chain with minimum mismatch.

IV. IMPLEMENTATION OF CHIRPLET CHAINS: CLUSTERING ALGORITHM

In order to better detect events with rapid frequency evolution that are extended in time, the chirplet clustering algorithm follows the strategy of chirplet chains proposed by [5]. Although the Omega hierarchical and density algorithms can cluster the output of the chirplet transform, they neither take into account chirprate nor the fact that clusters forming

chirp signals should resemble a chirplet chain with somewhat continuous phase evolution. The chirplet specific algorithm takes the thresholded pixels that have been obtained after the whitened data has been projected over the linearly variant frequency sin-gaussian template family with minimum mismatch as its input. These chirplet template *triggers* can be analyzed in order to assemble appropriate chirplet chains if they should exist. To do this, the chirplet clustering algorithm differs somewhat from the method described in [5].

The *regulatory parameters* defined in Equations (20a) and (20a) are replaced[2] with a set of three dimensionless parameters, along with two other conditions that govern whether a given set of tiles should be clustered to form a chirplet chain. The algorithm first sorts the triggers by start time. Next examine each tile j with duration σ_t, bandwidth σ_f, and chirprate d, and applies a set of conditions to its neighbor $j^{'}$ with duration $\sigma_t^{'}$, bandwidth $\sigma_f{}'$, and chirprate $d^{'}$, a time and frequency gap[3] away of Δt and Δf respectively (see Figure 4). In order to govern the maximum time gap , the measure δt is defined as

$$\delta t \equiv \frac{\Delta t}{\sigma_t + \sigma_t^{'}} \leq 0.05, \tag{21}$$

or the maximum time gap of two tiles can be at most $\frac{1}{20}$ their combined durations. In a similar way, governing the maximum frequency gap , the measure δf is defined by

$$\delta f \equiv \frac{\Delta f}{\sigma_f + \sigma_f^{'}} \leq 0.8, \tag{22}$$

or the maximum frequency gap of two tiles can be at most $\frac{4}{5}$ their combined bandwidths. A condition that the central frequency must increase is also applied. The measure δd defined by

$$\delta d \equiv \frac{d}{d'} \begin{cases} \leq 0.25 \\ \geq 1 \end{cases} \tag{23}$$

governs the chirprate ratios and implies that the maximum chirprate ratio of tile j to $j^{'}$ is 1:4 and the minimum ratio is 1:1. The condition that the chirprate must increase is also applied. The maximum difference in chirprates can be seen in Figure 5. A final step

[2] these "regulations", defined above, are motivated by the trigger response of chirplet to binary system coalescence injected waveforms

[3] although we use the term 'gap' , it refers to both the possibility of a positive or negative (overlaping) distance between two tiles j and $j^{'}$ in the time-frequency plane

of the algorithm decides, if there are multiple $j^{'}$ candidates that satisfy the conditions, to cluster the neighbor tile with the highest normalized tile energy in order to most increase the likelihood that the chirplet chain being constructed is a signal.

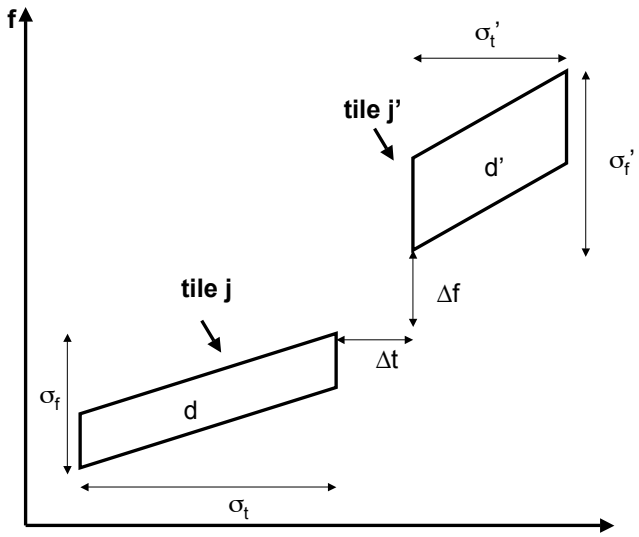

FIG. 4: Depiction of attempt form chirplet chain by clustering tile j to tile $j^{'}$

While linking chirplet triggers, the algorithm sums the tile energies for the chain, consequently increasing the likelihood that said chain is an event as it links together more tiles. A benefit of chirplet clustering is that the processes does not take into account trigger energy until a chirplet chain is already assured to exist, and it is simply deciding which tile is the best candidate to chose for the next link in the chain. Moreover, unless specified to do so, the algorithm does not recognize single pixels as events. As a result, the threshold for triggers to be considered by the chirplet clustering algorithm may be lowered and therefore could increase the sensitivity of the chirplet search to 'quieter' events. This, however, can only be done after the performance of the new algorithm is tested.

V. TESTING AND FUTURE WORK

In order to understand the whether the clustering algorithm works properly, a 'random number' test was first created. Triggers with pseudo random parameter values were created

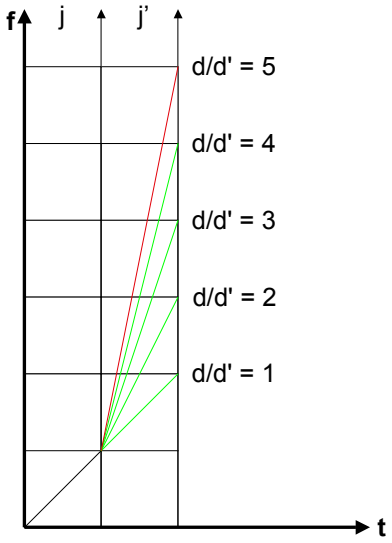

FIG. 5: Permisable chirprates are shown in green with the maximum ratio between j and j, being 1:4. The red line shows an increase that is too large.

in very large quantities using the matlab function *rand* in order to determined if the algorithm would cluster appropriately. The test has since been refined to produce more physical[5] random triggers. First, a number of tiles specified along with a density of tiles per unit time, which determines the length of the segment of trigger data. Next, random central times, τ, are assigned within that interval. Frequencies, chirprates, and quality factors are assigned in the ranges of $\phi \in (0, 1,000)$, $d \in (0, 2048)$, and $Q \in \left(\sqrt{11}, 100\right)$. From these values, the range of bandwidths can be calculated using Equation (8) as $\sigma_f \in (0, 10)$, and the durations can be calculated using the relation

$$\sigma_t = \frac{Q}{2\pi\sqrt{11}f} \tag{24}$$

as $\sigma_t \in \left(\frac{1}{2\pi}, \frac{50}{\sqrt{11}\pi}\right)$. Finally, the 'thresholded' normalized tile energies E are $E \in (0.5, 100)$. The test uses the new chirplet clustering algorithm to search for chirplet chains, and various

[5] these values were determined by standard parameter bounds for a chirplet search. Although they are not an exact representation of potential triggers that a chirplet search could produce from a stream of data because they are not discretized to the finite set of tiles in the signal space, they are a good approximation and resemble the general form of chirplet tiles

other parts of both chirplet and standard Omega to analyze and plot clusters in the time-frequency plane.

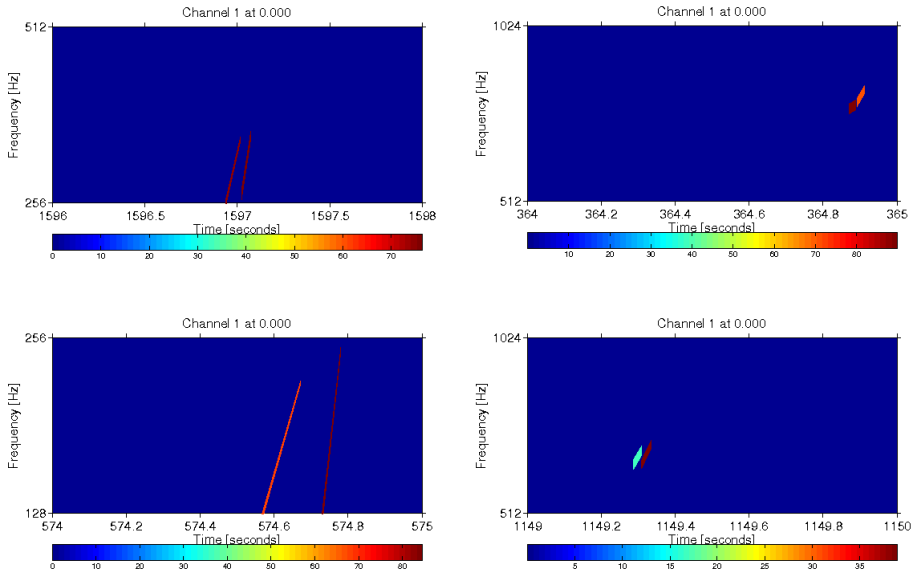

FIG. 6: Event grams of clustered reasonable random number events. No events exceeded 2 pixels even with 20,000 generated triggers distributed with uniform time density of 10 events per unit time.

Although the set of tests are not yet complete, we expect to learn a lot from its application. We are investigating at what time density of triggers is necessary to consistently produce clusters on a segment of fixed length. Moreover, it helps demonstrate the range of chirplet chains that the algorithm can output. The initial phase of tuning the dimensionless parameters can also start with this test. To see examples of chirplet chains produced by the clustering algorithm, see Figure 6. However, seeing as this does not use the chirplet search's tiling process, there are limits as to how much can be learned from it. Work has begun to run chirplet with the new clustering algorithm on Numerical INJection Analysis (NINJA) Project data. This data consists of either real detector data, or gaussian noise, injected with binary black hole coalescence waveforms of various sizes, spins, and alignments.

The performance of the algorithm on these tests will help determine whether the threshold discussed earlier may be lowered, and what other work must be done to finalize the new chirplet clustering algorithm.

Acknowledgements

The big bang, space-time, Einstein... Seriously, I would like to thank the many people without whom, I would not have had the privilege of working on this project in Paris this summer. First, I would like to thank Éric Chassande-Mottin for his continued guidance and patience. He has been an invaluable mentor throughout this processes. I would also like to thank Professor Bernard Whiting, Professor Guido Mueller, and the University of Florida Gainesville for their creation of and dedication to the truly one-of-a-kind Gravitational Waves International Research Experience for Undergraduates. Additionally, I owe great thanks to Professor Laura Cadonati of the University of Massachusetts Amherst who has invested a great deal in my education and research both at home and abroad. Her advice and guidance have and will continue to help me throughout my undergraduate career. I also greatly appreciate the substantial help I have received from Satya Mohapatra. His knowledge, direction, and assistance have been an extraordinary asset throughout my studies and research from Amherst to Paris. I would finally like to thank the NSF whose funding has made this experience possible. Without any of these people or entities, these memorable moments could not have happened:

FIG. 7: Sam and I at the Eiffel Tower

FIG. 8: My brother and I in front of Sacrè Coeur

References

[1] R. A. Hulse and J. H. Taylor, "Discovery of a pulsar in a binary system," Astrophys. J., vol. 195, pp. L51L53, 1975, 1975ApJ.195L.51H.

[2] J. H. Taylor, Binary pulsars and relativistic gravity, Rev. Mod. Phys., vol. 66, p. 711, 1994, 1994RvMP.66.711T.

[3] S. K. Chatterji. "The search for gravitational-wave bursts in data from the second LIGO science run". PhD thesis, MIT Dept. of Physics, 2005.

[4] Èric Chassande-Mottin *etal*, "Detection of GW bursts with chirplet-like template families," Class. Quantum Grav. 27 (2010) 194017

[5] Èric Chassande-Mottin and Archana Pai, "Best chirplet chain: Near-optimal detection of gravitational wave chirps," Phys. Rev D 73, 042004 (2006).

[6] `https://trac.ligo.caltech.edu/omega/browser/branches/chirplet`.

[7] P. Ajith et al. 'Complete' gravitational waveforms for black-hole binaries with non-precessing spins, 2009. arXiv:0909.2867.

[8] B. J. Owen and B. S. Sathyaprakash. Matched filtering of gravitational waves from inspiraling compact binaries: Computational cost and template placement. Phys. Rev., D60:022002, 1999. gr-qc/9808076.